Classification of Delayed Enhancement Scar Islands by Means of their Local Subendocardial Transmurality

Susana Merino-Caviedes[1], Lucilio Cordero-Grande[1], Teresa Sevilla[2], Teresa Pérez[3], Marcos Martín-Fernández[1], Carlos Alberola-López[1]

[1] Laboratorio de Procesado de Imagen, Universidad de Valladolid, Valladolid, Spain
[2] Servicio de Cardiología, Hospital Clínico Universitario, Valladolid, Spain
[3] Dpto. de Matemática Aplicada, Universidad de Valladolid, Valladolid, Spain

Abstract

Delayed Enhancement Magnetic Resonance (DE-MR) has clinical relevance in the diagnosis and prognosis of several cardiomyopathies with different etiologies, since they often lead to different scar configurations. However, to the best of our knowledge very little research has been devoted to the computational characterization of the scar islands detected by DE-MR and its location within the myocardial wall. Our purpose is to classify between subendocardial or transmural (S/T) scar islands and mid-wall or subepicardial (M/E) ones by means of their local subendocardial transmurality (LSTM).The results suggest that inspecting local magnitudes such as LSTM within isolated scar islands in DE-MR provides useful information with respect to the diagnosis of different types of cardiomyopathies and might help in the development of computer assisted diagnostic frameworks for nonischemic cardiomyopathies.

1. Introduction

Delayed Enhancement Magnetic Resonance (DE-MR) Imaging is a modality with established clinical applications, since it is able to detect damaged tissue within the myocardium. For its acquisition, a paramagnetic contrast bolus, which fills the myocardial intercellular space, is injected in the patient. After a few minutes the contrast washes out of the healthy tissue but still remains within the scar (infarcted tissue or fibrosis). The DE-MR volumes are then acquired, and show the scar as hyperenhanced regions.

In ischemic cardiopathy (ICM), the lack of blood supply damages firstly the tissue contiguous to the endocardium, as it is the furthest located from the coronary arteries that irrigate the myocardium. Then the damage propagates towards the epicardium in what is known as the ischemic wave front [1].

Nonischemic cardiomyopathies, on the other hand, do not originate from a coronary artery disease; they may appear due to several reasons, such as genetics, inflammation, infection, etc. Many of them show particular scar configurations that provide useful insight into their particular etiology. Among nonischemic cardiomyopathies, hypertrophic cardiomyopathy (HCM) is the most common cardiomyopathy of genetic origin, and leads in some cases to sudden death in young people [2]. This pathology presents an increased thickness of the left ventricle wall with a non-dilated blood cavity, and it is often accompanied by scar islands, located midwall at the left-right ventricle junctions.

The intramural location of the scar has relevance in the qualitative diagnosis of several cardiopathies. For example, it is well known that in ICM, the scar will have a subendocardial or transmural configuration, whereas the existence of midwall or subepicardial scar islands suggests a nonischemic origin for the cardiomyopathy (see Figure 1 in [3]). This is the case for HCM, myocarditis or sarcoidosis, among others. However, to the best of our knowledge there have been no efforts to develop automatic methods to automatically classify the scar with respect to its intramural configuration.

Many image-dependent markers in cardiology have been proposed; they typically provide average measures (of scar transmurality, strain, etc) on each of the myocardial sectors proposed in [4]. For the purpose of quantifying the intramural scar configuration, however, we propose to identify isolated scar islands on the myocardium and study the properties of each island regardless of sectors. In particular, a generalization of the transmural extent of the scar [5], which we designate here as the Local Subendocardial Transmurality (LSTM), yields good results on distinguishing between subendocardial and transmural (S/T) and midwall or subepicardial (M/E) scars, of probable ischemic and nonischemic origin respectively.The LSTM was submitted for consideration at the time the abstract

of this paper was written, and it is currently accepted for publication in [5], where a technical description, numerical implementation and validation of the LSTM by means of a Multi-Stencil Streamline Fast Marching method may be found. In this paper, we make use of it to build an automatic method that firstly, detects connected scar islands within the myocardium, and afterwards classifies them as S/T or M/E, with promising results.

The rest of the paper is organized as follows. In Section 2 a description of the methods used to implement the classifier is provided, while Section 3 details the experimental setup, results and discussion. In Section 4, some conclusions and future work are exposed.

2. Methods

2.1. Island identification

The first step in the proposed framework is the identification of the scar, for which a modification of the segmentation method proposed in [6] has been developed. This method requires a prior segmentation of both the endocardium and the epicardium, provided as binary masks. A preprocessing step is applied to the DE-MR volume and the endocardial and epicardial masks to overcome the difficulties that arise from the low interslice resolution in our DE-MR volumes. For this purpose, we use the topology-restricted interpolation algorithm developed by Cordero-Grande *et al.* [7], the output of which is a volume with a nearly isotropic voxel size. As in [6], the segmentation consists of three steps:

1. An initial segmentation is obtained by applying an intensity threshold on the myocardium. This threshold is automatically computed from the intensities of both the myocardium and the blood cavity.
2. After a connectivity analysis, the regions considered false positives due to either noise or delineation errors of the myocardial contours are removed. A minimum number of voxels is required so that the regions are not considered noise. In contrast to [6], the criterion to consider a region as a delineation error is based on the physical distance to the respective contour instead of on a ratio between interior and border voxels. This makes it more robust with respect to changes in resolution.
3. Then, false negatives are removed by region growing using the remaining regions as seed. Additionally with respect to [6], a hole filling step is applied to include microvascular obstructions in the final segmentation.

Finally, once the segmentation is obtained, a second connectivity analysis is performed to identify the remaining isolated scar islands.

2.2. Local subendocardial transmurality (LSTM)

Traditionally, the transmural extent of the myocardial scarred tissue (or transmurality) is a measure designed as a sector average of the ratio of the myocardial thickness covered by scar. Most of the existing methods use a ray-tracing methodology [8–10] to compute it on 2D slices of a short-axis acquisition. A high enough number of rays need to be traced through the myocardium, and for each of them, an individual transmurality measure is computed as the ratio of the amount of scar by the amount of myocardial tissue contained along the ray. Assuming the myocardium is divided into sectors (for example following the 17 segment model proposed in [4]), these individual measures are then averaged on each of them. However, these measures do not provide information on the intramural location of the scar.

The framework proposed in [5] redefines the concept of transmurality as a local measure that takes on values over the whole myocardium. It also provides a 3D method to compute a dense transmurality map which preserves information about the scar location within the myocardial wall, allowing at the same time to obtain sector transmurality values such as the ones yielded by the aforementioned current transmurality methods. The 3D transmurality map is computed in two steps. Firstly, a harmonic field $s(\mathbf{x})$ is computed by solving the Laplace equation between the endocardium and the epicardium, which provides a univocal mapping between both surfaces. Then, at each point $\mathbf{x}$ in the myocardium, the line integrals of the scar segmentation and the myocardial mask are computed over the streamline of $s(\mathbf{x})$ that crosses $\mathbf{x}$, between $\mathbf{x}$ and the endocardium, by means of the Multi-Stencil Streamline Fast Marching method (further details on its implementation can be found in [5]).

Figure 1 illustrates the behavior of the LSTM on three synthetic 1D scar profiles with the same myocardial thickness and global transmurality (of value 0.5), but with different spatial scar configuration. Figures 1(a), 1(b) and 1(c) show respectively subendocardial, midwall and subepicardial scar configurations, whose respective LSTM profiles are given in Figures 1(d), 1(e) and 1(f).

It may be observed that in the subendocardial configuration (Figures 1(a) and 1(d)) the LSTM takes unitary value while there is scar and decreases when it traverses healthy tissue, until it reaches the global transmurality value at the epicardium. In contrast, the LSTM of the subepicardial configuration (Figures 1(c) and 1(f)) has zero value from the endocardium until some scar is found, and then increases its value until it reaches the epicardium. As in the subendocardial configuration, the LSTM value at the epicardial border is the global transmurality. The LSTM

of the midwall scar configuration (Figures 1(b) and 1(e)) starts taking on a null value from the endocardium to the scar border, and then it starts to increase for as long as it traverses a scarred region. From there to the epicardium, the LSTM decreases and finally takes on the global transmurality value at the epicardium.

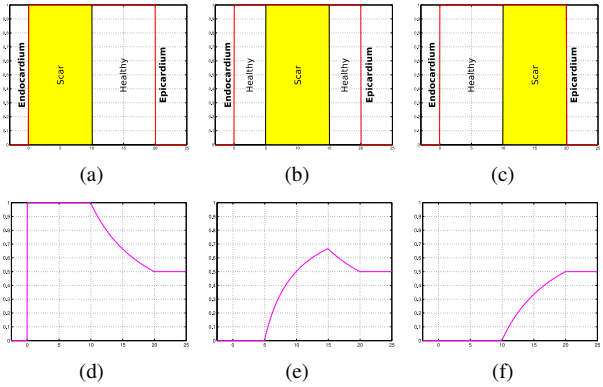

Figure 1. 1D profiles of a synthetic scar with a transmurality value of 0.5 with a (a) subendocardial, (b) midwall and (c) subepicardial configuration. (d), (e) and (f): their respective LSTM profiles.

2.3. Classification

Once the LSTM is computed within the whole myocardium and the scar islands are identified, the LSTM values and their histograms within each island are evaluated and normalized with respect to the number of voxels within the island. As Figure 1(d) suggests, the LSTM values on S/T islands are predominantly unitary, while in M/E scar the LSTM takes on values within a wider range (see Figures 1(e) and 1(f)). There was a marked difference between the normalized histograms of purely S/T and purely M/E islands; however, in many cases you may find islands whose configuration is a mixture of both of them.

Two sets of normalized histograms of S/T and M/E islands were chosen as centroids for the classifier. Then, each test normalized histogram was linearly correlated to every histogram of the training set, and it was classified as S/T or M/E depending on the class of the training histogram that yielded the highest correlation with the considered test histogram.

3. Experimental results

3.1. Datasets

For the development of this study we had access to 20 short-axis DE-MR volumes of patients with either an ICM or an HCM pathology, acquired with a 1.5T GE Genesis Signa MRI scanner. Each of them has between 3 and 13 slices with 10 mm of slice thickness. The in-plane spatial resolution varies among volumes, taking on values between 0.7031 mm and 1.6406 mm. After the topology-restricted interpolation, the slice thickness varied between 1.25 mm and 2.00 mm.

At the segmentation step, the required minimum size was set to 100 voxels, and the minimum distance to the myocardial contours to 2.00 mm. The island identification step yielded 30 islands were accepted for the training and testing sets, which were annotated as S/T or M/E by an expert. From them, a total of 5 islands were employed for training (2 S/T and 3 M/E) and 25 for testing.

3.2. Results

Since the LSTM does not follow a normal distribution, the paired Mann-Whitney U-test was performed between the S/T and M/E training islands. Its outcome indicated that their medians are different with p<1e-65.

The normalized histograms of the LSTM at each island are shown in Figure 2, each of them colored by their respective subset. The difference between the S/T (red) and the M/E (blue) train sets may be appraised, and how the shape of the histograms of the test sets varies between them.

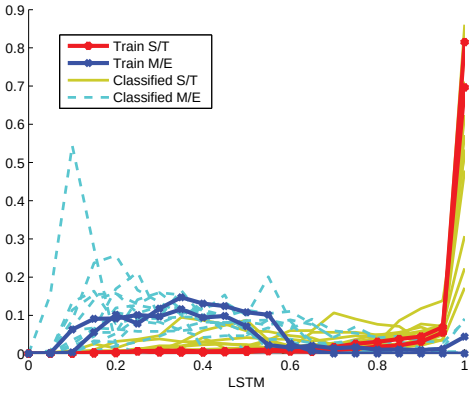

Figure 2. LSTM normalized histograms of the island set. The histograms in red and blue are used by the classifier to recognize S/T and M/E islands, respectively.

The classification results are shown in Table 1. The classifier achieved a success rate of 96%, with only one S/T island misclassified as M/E. The classification was repeated using a leave-one-out strategy, which only misclassified one island as well. The results suggest that the followed strategy provides a good interclass separability, allowing for simplicity in the classifier design. They also hint that the classifier is robust, in the sense that a well designed small training set may allow for variations in the scar configuration with a similar performance as using a larger

training set (with the subsequent computational economy).

Table 1. Performance of the classifier

	S/T_{expert}	M/E_{expert}
$S/T_{classif}$	12	0
$M/E_{classif}$	1	12

4. Conclusions and future work

In this work, a computational framework for the classification of connected myocardial scar islands depending on their intramural configuration is presented. This constitutes a first step towards developing a computer-aided tool for the diagnosis and risk stratification of nonischemic cardiomyopathies such as HCM using DE-MR. The proposed approach is based on a dense generalization of the transmural extent of the scar and inspecting the LSTM on the regions delimited by the existing connected myocardial scar islands, instead of on the 17 segment model of the myocardium. The classifier achieved an accuracy of 96% using only a small sample as training set.

Since our island dataset is relatively small, we plan to repeat our experiments with a larger bank of DE-MR volumes. This will allow to work towards the quantitative modelization of scar islands in HCM.

Acknowledgements

This work was partially supported by the Spanish Ministerio de Ciencia e Innovación and the Fondo Europeo de Desarrollo Regional under Research Grant TEC2010-17982, the Spanish Instituto de Salud Carlos III under Research Grant PI11–01492, and the European Commission under Research Grant FP7-223920 The work was also funded by the Spanish Junta de Castilla y León under Grants VA039A10–2, VA376A11-2, GRS 474/A/10, SAN103/VA40/11, SAN126/VA032/09 and SAN126/VA033/09.

References

[1] Reimer KA, Lowe JE, Rasmussen MM, Jennings RB. The wavefront phenomenon of ischemic cell death. 1. myocardial infarct size vs duration of coronary occlusion in dogs. Circulation 1977;56(5):786–94.

[2] Maron M. Clinical utility of cardiovascular magnetic resonance in hypertrophic cardiomyopathy. Journal of Cardiovascular Magnetic Resonance 2012;14(1):13.

[3] Karamitsos TD, Francis JM, Myerson S, Selvanayagam JB, Neubauer S. The role of cardiovascular magnetic resonance imaging in heart failure. Journal of the American College of Cardiology 2009;54(15):1407–1424.

[4] Heart Association Writing Group on Myocardial Segmentation and Registration for Cardiac Imaging: A, Cerqueira MD, Weissman NJ, Dilsizian V, Jacobs AK, Kaul S, Laskey WK, Pennell DJ, Rumberger JA, Ryan T, Verani MS. Standardized myocardial segmentation and nomenclature for tomographic imaging of the heart. Circulation 2002; 105(4):539–542.

[5] Merino-Caviedes S, Cordero-Grande L, Revilla-Orodea A, Sevilla-Ruiz T, Pérez MT, Martín-Fernández M, Alberola-López C. Multi-stencil streamline fast marching: a general 3D framework to determine myocardial thickness and transmurality in late enhancement images. IEEE Transactions on Medical Imaging Accepted;.

[6] Tao Q, Milles J, Zeppenfeld K, Lamb HJ, Bax JJ, Reiber JHC, van der Geest RJ. Automated segmentation of myocardial scar in late enhancement MRI using combined intensity and spatial information. Magnetic Resonance in Medicine 2010;64(2):586–594. ISSN 1522-2594.

[7] Cordero-Grande L, Vegas-Sanchez-Ferrero G, Casaseca-de-la Higuera P, Alberola-Lopez C. A Markov random field approach for topology-preserving registration: Application to object-based tomographic image interpolation. IEEE Transactions on Image Processing 2012;21(4):2047–2061. ISSN 1057-7149.

[8] Schuijf JD, Kaandorp TAM, Lamb HJ, van der Geest RJ, Viergever EP, van der Wall EE, de Roos A, Bax JJ. Quantification of myocardial infarct size and transmurality by contrast-enhanced magnetic resonance imaging in men. American Journal of Cardiology 2004;94(3):284–288.

[9] Nazarian S, Bluemke DA, Lardo AC, Zviman MM, Watkins SP, Dickfeld TL, Meininger GR, Roguin A, Calkins H, Tomaselli GF, Weiss RG, Berger RD, Lima JAC, Halperin HR. Magnetic resonance assessment of the substrate for inducible ventricular tachycardia in nonischemic cardiomyopathy. Circulation 2005;112(18):2821–2825.

[10] Elnakib A, Beache G, Gimel'farb G, El-Baz A. New automated Markov–Gibbs random field based framework for myocardial wall viability quantification on agent enhanced cardiac magnetic resonance images. The International Journal of Cardiovascular Imaging formerly Cardiac Imaging 2012;28:1683–1698.

Address for correspondence:

Susana Merino-Caviedes
Laboratorio de Procesado de Imagen
E.T.S.I. de Telecomunicación
Paseo de Belén 15, 47011
Valladolid, Spain
smercav@lpi.tel.uva.es